# A Fault Tolerant Selective Harmonic Elimination Method for Modular Multilevel Converters

Ardavan Mohammadhassani and Ali Mehrizi-Sani
The Bradley Department of Electrical and Computer Engineering
Virginia Tech
Blacksburg, VA 24060
Emails: {ardavanmh93,mehrizi}@vt.edu

Abstract—A selective harmonic elimination pulse-width modulation (SHE-PWM) is proposed in this paper for adding fault tolerant capabilities to the operation of modular multilevel converters (MMC). This method maintains the fundamental harmonic of the faulty phase voltage during single submodule failures in order to keep the line-to-line voltages balanced. A circulating current controller is also designed to mitigate the ac component of the circulating currents while keeping the predefined shape of the output voltage. A 9-level MMC model is built in PSCAD/EMTDC to verify the advantages of the proposed method.

Index Terms—Harmonic suppression, modular multilevel converters, fault tolerant control, model predictive control

#### I. INTRODUCTION

The modular multilevel converter (MMC) has become an attractive topology for various applications due to its voltage and power scalability and higher power quality [1]. The multilevel operation of the MMC and its advantages are enabled by the presence of a number submodules (SM) in each of its phases. On the other hand, utilization of SMs increases the chance of SM failure and reduces the reliability of the MMC. Thus, it is crucial that the MMC has fault tolerant (FT) capabilities to maintain its normal operation during SM faults.

FT methods based on using redundant SMs are proposed in [2], [3]. In these methods, redundant SMs are inserted as soon as the faulty SM is located and bypassed. Thus, the MMC can maintain its normal operation. The method in [2] utilizes cold redundant SMs. In this case, the converter operation will suffer from long charging periods and transient problems. This problem was solved in [3] by charging the redundant SMs during the normal operation of the MMC. However, this will complicate the control of the converter and increase the switching losses.

Switching from hardware-based methods to software-based methods, modified modulation techniques can also be utilized for enabling FT operation of the MMC. The method proposed in [4] is probably the only method that purely modifies the modulation scheme for achieving FT operation of the MMC. In this method, a modified space vector modulation is proposed for providing FT capability alongside circulating current suppression and capacitor voltage balancing.

Another attractive modulation method is the selective harmonic elimination pulse-width modulation (SHE-PWM). The main principle in SHE-PWM is to design the output voltage

reference waveform such that certain low-order harmonic are eliminated and the fundamental harmonic is controlled. SHE-PWM has been formulated and applied for the MMC in [5].

In addition to modifying SHE-PWM for FT operation, a circulating current controller needs to be designed. This is due to the fact that previous circulating current controllers [6] will degrade the output voltage of the MMC due to variable distances between the switching times of SHE-PWM. In addition, these methods apply different modulation indices for different phases which will increase the amplitude of the low-order harmonics of the phase voltages. A method is introduced in [5] that controls the circulating current between two bounds while preserving the designed shape for the output voltage. However, this method inserts additional switching commands for controlling the circulating which increases the switching losses of the MMC.

In this paper, a modified SHE-PWM is introduced for the MMC to provide FT capabilities. This method maintains the fundamental harmonic during single SM failures. Thus, the line-to-line voltages will be balanced. The SHE-PWM waveforms are designed and the switching angles are found by solving the SHE-PWM equations using exchange market algorithm for both normal and abnormal operating conditions [7]. In addition, a circulating current controller is proposed for operating along with SHE-PWM without degrading the output voltage and increasing the switching losses. This method is based on weighted model predictive control [8], [9]. The benefits of the proposed method are verified on a 9-level three-phase MMC model built in PSCAD/EMTDC.

The rest of this paper is structured as follows. Section II investigates the modified SHE-PWM for the MMC. The proposed circulating current controller is investigated in Section III. Simulation results are presented in Section IV. Finally, conclusions are presented in Section V.

#### II. FT SHE-PWM

In this paper, the output voltage reference waveforms are designed based on the 2N+1 SHE-PWM concept proposed in [5]. For instance, the designed output voltage waveform of phase a during normal operation is shown in Fig. 1. The voltage levels are denoted by  $0, 0.5V_c, ..., 2V_c$ , where  $V_c$  is the rated capacitor voltage of a single SM. There are 15 switching angles which are demonstrated by  $\alpha_1, \alpha_2, ..., \alpha_{15}$ .

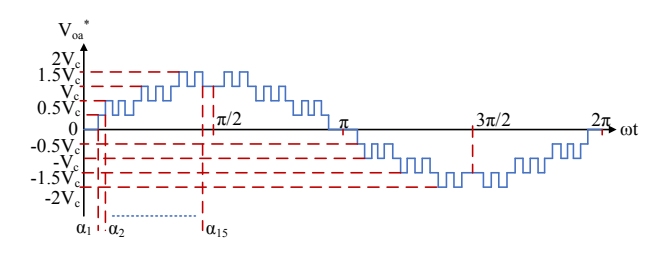


Fig. 1. Designed 2N+1 SHE-PWM waveform for phase a of a 9-level MMC.

The SHE-PWM equations can be derived using the Fourier expansion of the waveform shown in Fig. 1. The Fourier expansion of the waveform  $V_{an}(\omega t)$  can be written as:

$$V_{an}(\omega t) = \sum_{n=1}^{\infty} b_n \sin(\omega t)$$
 (1)

where  $b_n$  is defined as:

$$b_n = \frac{2V_{dc}}{n\pi N} \sum_{m=1}^{15} n_m \cos(n\alpha_m)$$
 (2)

where N is the number of SMs in each phase arm, and  $n_m$  is +1 for rising step and -1 for falling step.

In this paper, low-order harmonics from 5th harmonic up to the 13th harmonic are set to be eliminated while the fundamental harmonic is maintained at the reference value. The SHE-PWM system of equations for normal operating conditions are derived as:

$$V_{a1n} = \frac{3M_n V_{dc}}{2\pi} \tag{3}$$

$$\sum_{m=1}^{15} n_m \cos(n\alpha_m) = 0 \tag{4}$$

where n = 5, 7, 9, 11, 13 and  $M_n$  is the modulation index which is defined as:

$$M_n = \frac{2\pi V_{a1n}^*}{3V_{dc}}, 0 < M_n < 1 \tag{5}$$

The designed 2N+1 SHE-PWM waveform for phase a of a 9-level MMC during single SM failure is shown in Fig. 2. When a single SM fails, the faulty phase will generate a 7-level voltage waveform instead of a 9-level. The waveform has 14 number of switching angles.

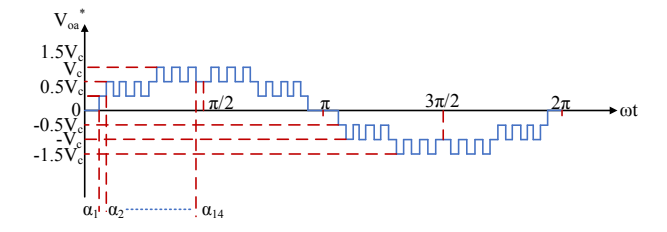


Fig. 2. Designed 2N+1 SHE-PWM waveform for phase a of a 9-level MMC during single SM failure.

The SHE-PWM equations for the designed waveform during single SM failure are written as:

$$V_{a1f} = \frac{4M_f V_{dc}}{3\pi} \tag{6}$$

$$\sum_{m=1}^{15} n_m \cos(n\alpha_m) = 0 \tag{7}$$

where, n = 5, 7, 9, 11, 13 and  $M_f$  is the modulation index for SHE-PWM during single SM failure.  $M_f$  is written as:

$$M_f = \frac{3\pi V_{a1f}^*}{4V_{dc}}, 0 < M_f < 1 \tag{8}$$

In this paper, the FT operation of the MMC is enabled by keeping the fundamental harmonic of the faulty phase voltage equal to its pre-fault value. This is done via manipulating the modulation index during the fault conditions. If we set (3) equal to (6), the relationship between  $M_n$  and  $M_f$  can be found as

$$M_f = \frac{9}{8}M_n \tag{9}$$

Thus, by calculating  $M_f$  from (9) during fault conditions, the fundamental harmonic of the faulty phase voltage is maintained and equal to that of the healthy phase voltages. Hence, the line-to-line voltages will be kept balanced during fault conditions.

The switching angles for normal operation of the converter are shown in Fig. 3. Switching angles for FT operation of the MMC are plotted in Fig. 4.

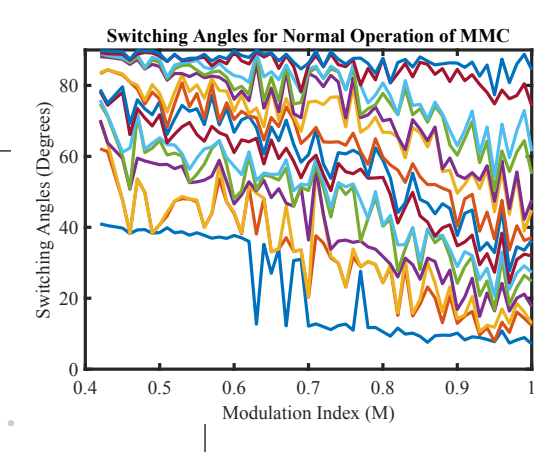


Fig. 3. Switching angles for normal operating conditions.

# III. CIRCULATING CURRENT CONTROL

## A. A Brief Overview of MMC Operation

The generic topology of a three-phase MMC is shown in Fig. 5. This topology consists of three phase legs with upper and lower arms in each leg. Each phase arm consists of N half-bridge SMs. The upper and lower arm currents are denoted by  $I_{ui}$  and  $I_{li}$ , upper and lower arm voltages by  $V_{ui}$  and  $V_{li}$ , and output phase voltages and currents are by  $V_{oi}$  and  $I_{oi}$ , where i=a,b,c.

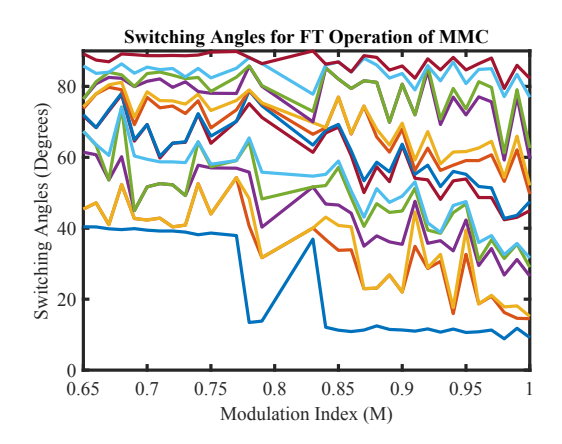


Fig. 4. Switching angles for FT operating conditions.

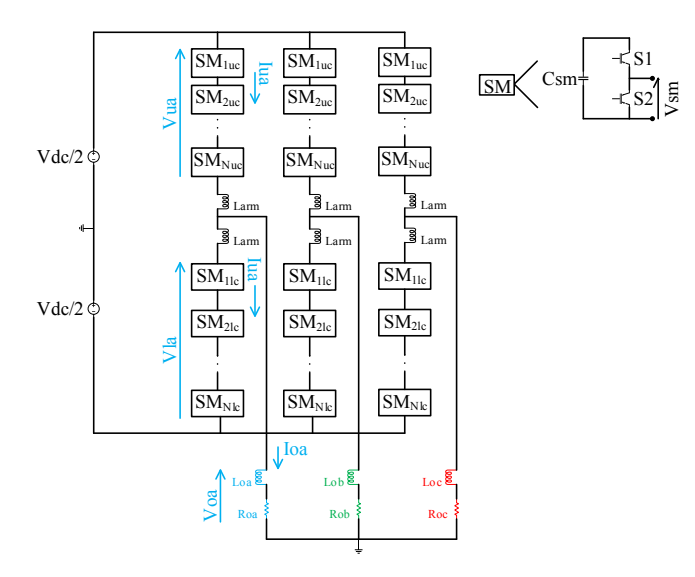


Fig. 5. Generic topology of a three-phase MMC.

The output phase voltages  $V_{oi}$  and circulating currents  $I_{ci}$  are found as

$$V_{oi} = \frac{V_{li} - V_{ui}}{2} \tag{10}$$

$$\frac{dI_{ci}}{dt} = \frac{V_{dc} - V_{ui} - V_{li}}{2L_{arm}} \tag{11}$$

The upper and lower arm voltages  $V_{ui}$  and  $V_{li}$  at each time instant are written using the upper and lower arm insertion indices  $n_{ui}$  and  $n_{li}$  as

$$V_{ui}(t) = n_{ui}(t) \sum_{h=1}^{N} V_{C_{SM}}(t)$$
 (12)

$$V_{li}(t) = n_{li}(t) \sum_{k=1}^{N} V_{C_{SM}}(t)$$
 (13)

## B. Proposed Circulating Current Controller

In this paper, the weighted model predictive control principle [9] is utilized to design the circulating current controller. WMPC determines which insertion index is optimum for generating the designated voltage level according to the cost function below

$$Cost = \sqrt{f_1^2 + f_2^2 + f_3^2}$$
 (14)

where  $f_1$ ,  $f_2$ , and  $f_3$  are defined as

$$f_{1} = \left(\frac{I_{ci}(n+1) - I_{ci}^{*}}{g_{1}}\right)^{2}$$

$$f_{2} = \left(\frac{V_{ui}(n) - n_{ui}(n)V_{dc}}{g_{2}}\right)^{2}$$

$$f_{3} = \left(\frac{V_{li}(n) - n_{li}(n)V_{dc}}{g_{3}}\right)^{2}$$
(15)

where,  $g_1^{\dagger}$ ,  $g_2$ , and  $g_3$  are weighting factors which are determined by trial and effort, and  $I_{ci}(n+1)$  is the predicted value of  $I_{ci}$  for the next sampling instant. This value is found by discretizing (20)

$$I_{ci}(n+1) = \frac{T_s(V_{dc} - V_{ui}(n+1) - V_{li}(n+1))}{2L_{arm}} + I_{ci}(n)$$
(16)

Finally, the insertion indices are sent to the submodule sorting algorithm to generate the gating signals and balance the capacitor voltages.

## IV. SIMULATION RESULTS

#### A. MMC Operation During Normal Conditions

A 9-level MMC with N=4 is modeled in PSCAD/EMTDC for simulation purposes. Converter parameters are summarized in Table. I.

TABLE I SIMULATION PARAMETERS

Parameter	Value
DC Voltage	$10 \ kV$
Load Resistance, $R_{oi}$	12 Ω
Load Inductance, $L_{oi}$	4~mH
Arm Inductance, $L_{arm}$	9~mH
SM Capacitance, $C_{SM}$	$4600 \ \mu F$
MPC Sampling Frequency, $f_s$	2 kHz
Nominal SM Voltage, $V_{c_{SM}}$	2.5~kV

The simulated line-to-neutral voltage of phase a,  $V_{an}$ , and line-to-line voltage,  $V_{ab}$ , during normal operating conditions for  $M_n=0.8$  are plotted in Fig. 6 and Fig. 7. Both voltages follow their respective reference waveforms.

The harmonic spectrums of  $V_{an}$  and  $V_{ab}$  are plotted in Fig. 8 and Fig. 9. All of the undesired harmonics are eliminated and the fundamental harmonic is controlled.

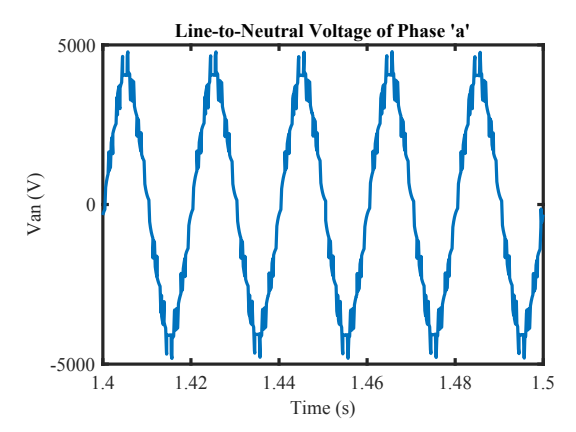


Fig. 6. Simulated line-to-neutral voltage of phase a.

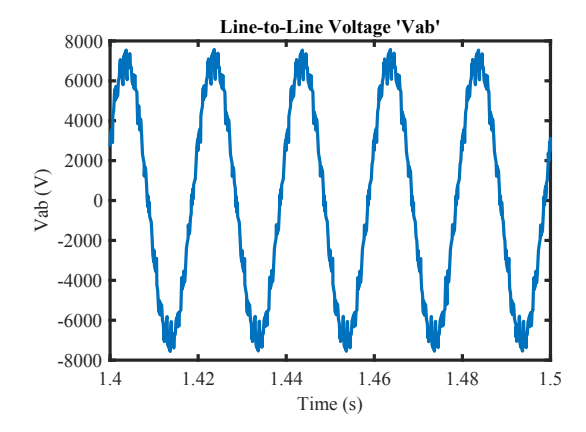


Fig. 7. Simulated line-to-line voltage  $V_{ab}$ .

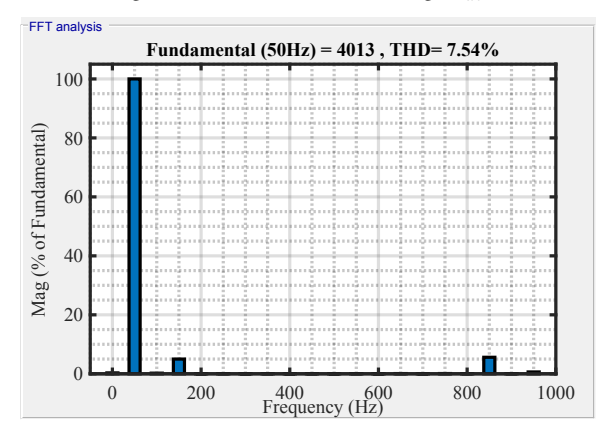


Fig. 8. Harmonic spectrum of  $V_{an}$ .

The circulating current of phase a is plotted in Fig. 10. It can be seen that the proposed controller was successful in controlling the ac component of the circulating current without disturbing the output voltages.

#### B. FT Operation of MMC

At t=1.5,  $SM_{1ua}$  fails and is bypassed using a SCR. In this case, there are 3 SMs in the upper arm of phase a and 4 SMs in the lower arm. The modulation index for FT operation is found to be  $M_f=0.9.\ V_{an}$  and  $V_{ab}$  during FT operation

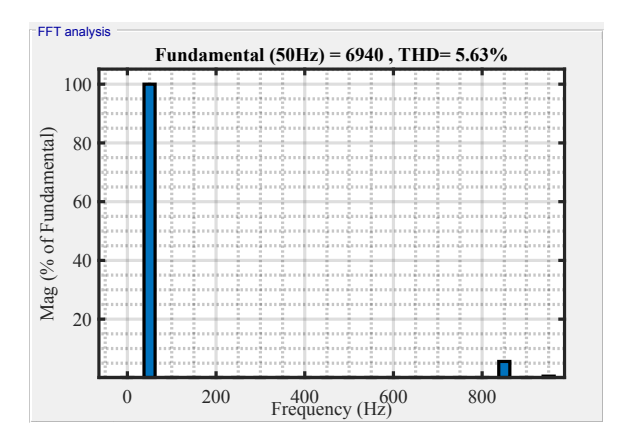


Fig. 9. Harmonic spectrum of  $V_{ab}$ .

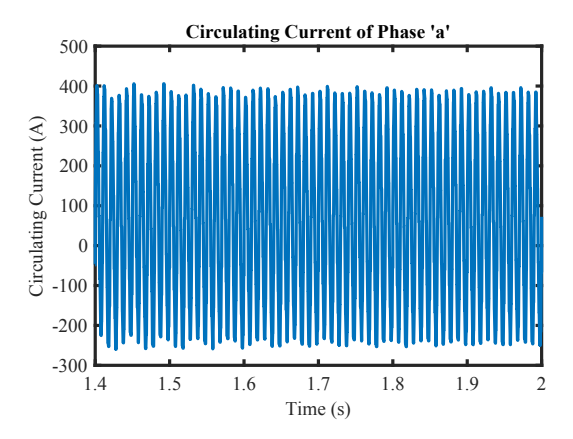


Fig. 10. Circulating current of phase a during normal operation.

are shown in Fig. 11 and Fig. 12. The voltages follow their reference waveforms. In addition, the harmonic spectrums of  $V_{an}$  and  $V_{ab}$  are plotted in Fig. 13 and Fig. 14. They shows that the fundamental harmonic is maintained and low order harmonics are controlled. Thus, FT operation is achieved. The circulating current during FT operation is shown in Fig. 15. Once again, the ac components of the circulating current is controlled without degrading the output voltages.

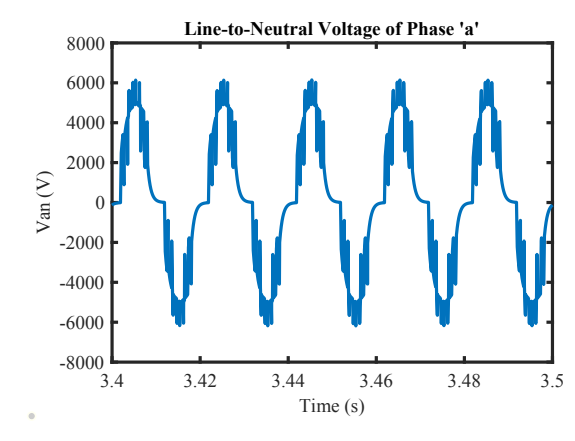


Fig. 11. Line-to-neutral voltage of phase a during single SM failure.

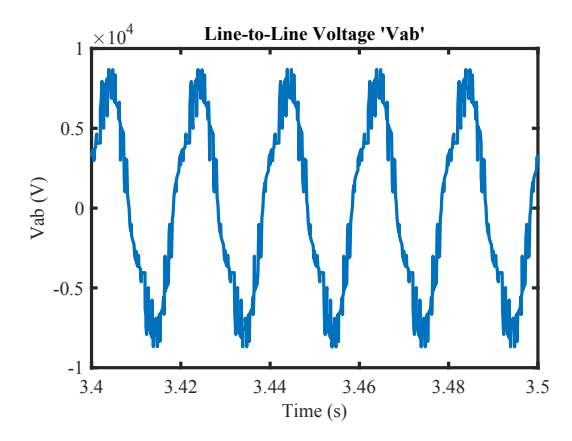


Fig. 12. Simulated line-to-line voltage  $V_{ab}$  during single SM failure.

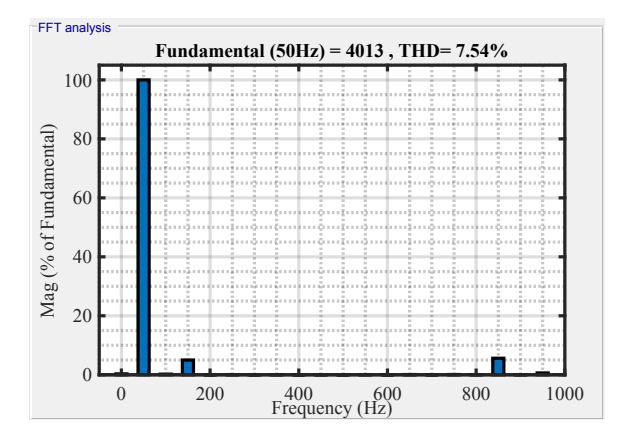


Fig. 13. Harmonic spectrum of  $V_{an}$  during single SM failure.

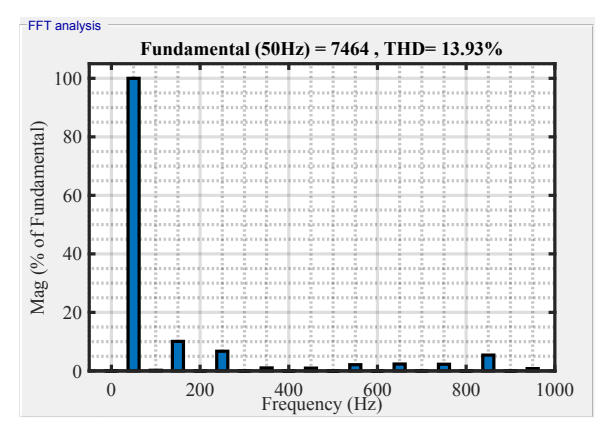


Fig. 14. Harmonic spectrum of  $V_{ab}$  during single SM failure.

### V. CONCLUSION

A fault tolerant selectvie harmonic elimination method was proposed in this paper along with a circulating current controller based on weighted model predictive control. The proposed fault tolerant method maintains the fundamental harmonics during single submodule failure to keep the line-to-line voltages balanced while the circulating current controller controls the circulating currents without degrading the output voltage. The proposed method does not require redundant submodules. Thus, the MMC will be cheaper and smaller

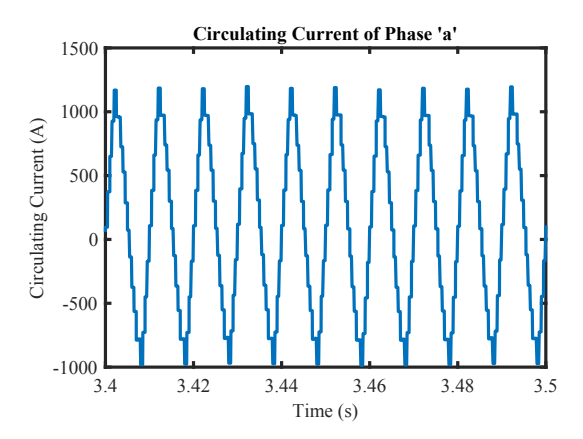


Fig. 15. Circulating current of phase a during single SM failure.

in size and it will not suffer from charging transients. The proposed method was investigated via simulations on a 9-level MMC in PSCAD/EMTDC. Simulation results prove the proposed advantages.

#### REFERENCES

- S. Debnath, J. Qin, B. Bahrani, M. Saeedifard, and P. Barbosa, "Operation, control, and applications of the modular multilevel converter: A review," *IEEE Trans. Power Electron.*, vol. 30, no. 1, pp. 37–53, Jan 2015.
- [2] G. Liu, Z. Xu, Y. Xue, and G. Tang, "Optimized control strategy based on dynamic redundancy for the modular multilevel converter," *IEEE Trans. Power Electron.*, vol. 30, no. 1, pp. 339–348, Jan 2015.
- [3] S. Yang, Y. Tang, and P. Wang, "Seamless fault-tolerant operation of a modular multilevel converter with switch open-circuit fault diagnosis in a distributed control architecture," *IEEE Trans. Power Electron.*, vol. 33, no. 8, pp. 7058–7070, Aug 2018.
- [4] M. Aleenejad, H. Mahmoudi, S. Jafarishiadeh, and R. Ahmadi, "Fault-tolerant space vector modulation for modular multilevel converters with bypassed faulty submodules," *IEEE Trans. Ind. Electron.*, vol. 66, no. 3, pp. 2463–2473, March 2019.
- [5] A. Pérez-Basante, S. Ceballos, G. Konstantinou, J. Pou, J. Andreu, and I. M. de Alegría, "(2n+1) selective harmonic elimination-pwm for modular multilevel converters: A generalized formulation and a circulating current control method," *IEEE Trans. Power Electron.*, vol. 33, no. 1, pp. 802–818, Jan 2018.
- [6] S. Yang, P. Wang, Y. Tang, M. Zagrodnik, X. Hu, and K. J. Tseng, "Circulating current suppression in modular multilevel converters with even-harmonic repetitive control," *IEEE Trans. Ind. Appl.*, vol. 54, no. 1, pp. 298–309, Jan 2018.
- [7] A. MohammadHassani and E. Babaei, "Exchange market algorithm for selective harmonic elimination in cascaded multilevel inverters," in 13th International Conference on Theory and Application of Fuzzy Systems and Soft Computing — ICAFS-2018, 2019, pp. 594–601.
- [8] A. M. Hassani, S. I. Bektas, and S. H. Hosseini, "Modular multilevel converter circulating current control using model predictive control combined with genetic algorithm," *Procedia Computer Science*, vol. 120, pp. 780 787, 2017, 9th International Conference on Theory and Application of Soft Computing, Computing with Words and Perception, ICSCCW 2017, 22-23 August 2017, Budapest, Hungary.
- [9] L. Ben-Brahim, A. Gastli, M. Trabelsi, K. A. Ghazi, M. Houchati, and H. Abu-Rub, "Modular multilevel converter circulating current reduction using model predictive control," *IEEE Trans. Ind. Electron.*, vol. 63, no. 6, pp. 3857–3866, June 2016.